Journal of Power Sources 195 (2010) 21–29

Contents lists available at ScienceDirect

Journal of Power Sources

journal homepage: www.elsevier.com/locate/jpowsour

Radiation-grafted membranes based on polyethylene for direct methanol fuel cells☆

Tauqir A. Sherazi[a,b], Michael D. Guiver[b,*], David Kingston[b], Shujaat Ahmad[c], M. Akram Kashmiri[a,d], Xinzhong Xue[b]

[a] Department of Chemistry, Government College University, Lahore 54000, Pakistan
[b] Institute for Chemical Process and Environmental Technology, National Research Council Canada, 1200 Montreal Road, Ottawa, ON K1A 0R6, Canada
[c] PIEAS/PINSTECH, P O Nilore, Islamabad 45650, Pakistan
[d] Board of Intermediate and Secondary Education, Lahore 54000, Pakistan

ARTICLE INFO

Article history:
Received 27 April 2009
Received in revised form 10 July 2009
Accepted 10 July 2009
Available online 21 July 2009

Keywords:
Fuel cell
Proton exchange membrane
Radiation grafting
Polyethylene
Membrane–electrode assembly

ABSTRACT

Styrene was grafted onto ultrahigh molecular weight polyethylene powder (UHMWPE) by gamma irradiation using a ^{60}Co source. Compression moulded films of selected pre-irradiated styrene-grafted ultrahigh molecular weight polyethylene (UHMWPE-g-PS) were post-sulfonated to the sulfonic acid derivative (UHMWPE-g-PSSA) for use as proton exchange membranes (PEMs). The sulfonation was confirmed by X-ray photoelectron spectroscopy (XPS). The melting and flow properties of UHMWPE and UHMWPE-g-PS are conducive to forming homogeneous pore-free membranes. Both the ion conductivity and methanol permeability coefficient increased with degree of grafting, but the grafted membranes showed comparable or higher ion conductivity and lower methanol permeability than Nafion® 117 membrane. One UHMWPE-g-PS membrane was fabricated into a membrane–electrode assembly (MEA) and tested as a single cell direct methanol fuel cell (DMFC). Low membrane cost and acceptable fuel cell performance indicate that UHMWPE-g-PSSA membranes could offer an alternative approach to perfluorosulfonic acid-type membranes for DMFC.

1. Introduction

Fuel cells are electrochemical devices that convert chemical energy directly into electricity, and are regarded as one of the promising clean future power sources. The proton exchange membrane fuel cell (PEMFC) and direct methanol fuel cell (DMFC), which use polymeric proton conductive membranes as one of the key components, are drawing increasing attention for their utility in automotive and portable applications [1,2]. Of these two PEMFC systems, DMFC is advantageous for portable power applications, primarily because it avoids the difficulties of storing hydrogen and because of the relatively good electrochemical reactivity of methanol (although it is far below that of hydrogen). It is of interest to operate DMFCs under a variety of operating conditions depending on specific system requirements (methanol concentration, flow rate, humidification, cell temperature, operating voltage or current, etc.), in order to improve efficiency. Today, commercially available DMFCs (e.g. Antig, MTI Micro, SFC Smart Fuel Cell AG) are based on Nafion® membranes or similar perfluorosulfonic acid (PFSA) membranes because they exhibited a number of desirable properties, such as high ionic conductivity, mechanical strength, and chemical/thermal stability. However, high cost, limited operation temperature ($\leq$80 °C), high methanol crossover, and environmental recycling uncertainties of Nafion® and other PFSA membranes are limiting their widespread commercial application in fuel cell systems [3,4].

Therefore, a concerted effort is being made to develop new high-performance proton conductive membranes as an alternative to commercially available PFSA membranes. These efforts were generally divided into two categories. The first is to modify the Nafion® membranes by surface treatment or by blending them with other polymers or inorganic materials, primarily in an attempt to reduce methanol permeability. Nafion®/silica composites [5,6] and Nafion®/poly(vinylidene fluoride hexafluoropropylene) blended membranes [7] are good examples of this category. The second is to develop new synthetic polymeric membranes that have ionic clusters with a smaller percolation size compared with Nafion®. These include sulfonated derivatives of poly(ether sulfone) (SPES) [8,9], poly(ether ether ketone) (PEEK) [2,10], polyimide (SPI) [11,12], polyimidazole [13], poly(aryl ether) [14,15], polyphenylene [16,17], polybenzimidazole [18], hybrid membranes [19] and radiation-grafted membranes [20–22].

☆ NRCC Publication No. 51718.

* Corresponding author. Tel.: +1 613 993 9753; fax: +1 613 991 2384.
E-mail address: michael.guiver@nrc-cnrc.gc.ca (M.D. Guiver).

0378-7753/$ – see front matter.
doi:10.1016/j.jpowsour.2009.07.021

The large percolation size of PFSA membranes is an advantage, being the source of high proton conductivity. Unfortunately, at the same time it is also the source of higher methanol crossover, which is the major limitation of PFSA membranes in the DMFC application. Thus methanol transport and proton conductivity have somewhat of a trade-off relationship in that it is difficult to selectively reduce one without affecting the other and vice versa [23]. In general, hydrocarbon or partially fluorinated membranes possess considerably lower methanol permeability, which allows the corresponding DMFC to be operated with relatively higher methanol concentration. Ultrahigh molecular weight polyethylene (UHMWPE) is an inexpensive material with high crystallinity that offers an excellent combination of properties in terms of chemical inertness and good mechanical strength, which made UHMWPE the material of choice in a number of applications. However, UHMWPE-based PEMs have not been reported yet for the evaluation of DMFC performance.

The present study is focused on the evaluation of an inexpensive hydrocarbon polymer electrolyte membranes based on radiation induced styrene-grafted onto UHMWPE. A ^{60}Co gamma source was used for irradiation. The prepared proton exchange membranes were characterized by X-ray photoelectron spectroscopy (XPS), and surface analyses were performed by using SEM. Proton conductivity and methanol permeability are also presented and compared with Nafion® 117. A selective membrane was also assessed for DMFC performance.

2. Experimental

2.1. Materials

Styrene-grafted UHMWPE (UHMWPE-g-PS) films used were prepared by the author as described in our previous paper [24]. Chlorosulfonic acid ($ClSO_3H$) sulfonating agent and dichloroethane solvent were obtained from Sigma–Aldrich. Analytical grade dichloromethane was obtained from EMD Ltd. All chemicals were used as received.

2.2. Radiation grafting

Methanol-washed and vacuum dried UHMWPE powder was used for irradiation. To carry out irradiation, UHMWPE powder was placed in screw-cap air-tight glass vials sealed with rubber septa, each vial containing 2.0 g of UHMWPE powder. Ar gas was used to create inert atmosphere. The vials were then inserted into the irradiation chamber, where the irradiation was carried out to obtain 5 kGy absorbed dose in Ar atmosphere. The ^{60}Co source was used for γ-irradiation at a calibrated dose rate of 649 Gy h^{-1} and the source was supplied by MDS Nordion, Canada. Solutions of styrene monomer were added to the pre-irradiated samples of UHMWPE powder and maintained at 60 °C for 24 h. Monomer concentrations were varied from 10 to 40% by volume in toluene solvent, leading to the UHMWPE samples having a final degree of grafting (*DG*) ranging from 12 to 44%. Following the styrene-grafting reactions, the polymers were washed and dried under vacuum until constant weight was reached. The degree of grafting was obtained by using the following equation

$$\text{Degree of grafting}\,(\%) = \frac{W_g - W_o}{W_o} \times 100 \quad (1)$$

where W_o and W_g are the weights before and after the grafting reaction, respectively.

2.3. Sulfonation

Styrene-grafted UHMWPE powder was converted into films by a compression moulding technique. For this purpose, measured amounts of grafted UHMWPE powder were pressed between two thin stainless steel plates using 6000 psi pressure at a set plate temperature of 220 °C for 10 min. The detailed description of the film forming procedure is presented elsewhere [24]. Sulfonation of the UHMWPE-g-PS films was carried out by directly immersing the film in a 0.2 M chlorosulfonic acid solution of dichloroethane for 5 h at 50 °C, then overnight at room temperature. After sulfonation, the membranes were removed from sulfonating solution and immersed in fresh dichloromethane for 3 h followed by washing with dichloromethane for removal of residual acid. After washing with dichloromethane, the films were thoroughly washed with deionized water.

The ion exchange capacity (*IEC*) of the sulfonated polymers was measured using a typical titration method. The *IEC* was calculated using the following equation

$$IEC_{exp} = \frac{0.05 \times V_{NaOH}}{W_{dry}} (\text{mequiv. g}^{-1}) \quad (2)$$

where V_{NaOH} (mL) is the volume of the 0.05 M NaOH solution used for titration. W_{dry} (g) is the dry weight of the polymer electrolyte membrane in the protonic form.

2.4. XPS analysis

The samples were analyzed, using the Kratos Axis Ultra X-ray photoelectron spectrometer (XPS) equipped with a non-monochromated Al X-ray source. Three analyses were performed on each sample to ensure reproducibility. Analyses were carried out using an accelerating voltage of 14 kV and a current of 10 mA. Charge build-up was compensated for using the Axis charge balancing system. The pressure in the analysis chamber during analysis was 2.0×10^{-9} Torr. Survey scans were carried out in the binding energy range of 1100–0 eV and pass energy of 160 eV to identify all the species present. High resolution scans were performed for C 1s, O 1s and S 2p regions at pass energy of 40 eV. Peak assignments were based on the NIST database (http://srdata.nist.gov/xps/Bind_E.asp), High Resolution XPS of Organic Polymers [25] and relevant publications. Peak fitting was performed using CasaXPS (ver. 2.2.107) data processing software. Shirley background correction procedures were used as provided by CasaXPS. Curve fitting procedures used for high resolution spectra presented in this paper used a Gaussian–Lorentzian (30) function. High resolution analyses were calibrated to adventitious C 1s signal, at 285 eV. Quantification was performed using sensitivity factors provided by CasaXPS's Scofield element library.

2.5. Scanning electron microscope (SEM) studies

Scanning electron microscopy (SEM, LEO 440, UK, magnification = 5× to 300,000×, resolution = 3.5 nm) was used for the morphological analysis of the sulfonated and non-sulfonated samples. For SEM analysis, small pieces of UHMWPE, UHMWPE-g-PS and UHMWPE-g-PSSA samples were pasted onto aluminum stubs with silver paste. Once the paste was dry the films were coated with a thin layer of gold (Au) by a sputtering technique using a Magnetron sputtering device (MSD). The gold-coated samples were placed in the SEM sample chamber and analyzed at a magnification of 2500×. The detector used was a secondary electron (SE) detector.

2.6. Proton conductivity

Proton conductivity measurements of the UHMWPE-g-PSSA membranes were derived from AC impedance spectroscopy measurements over a frequency range of 1–10^7 Hz using a system based on a Solatron 1260 gain phase analyzer. Each membrane sample

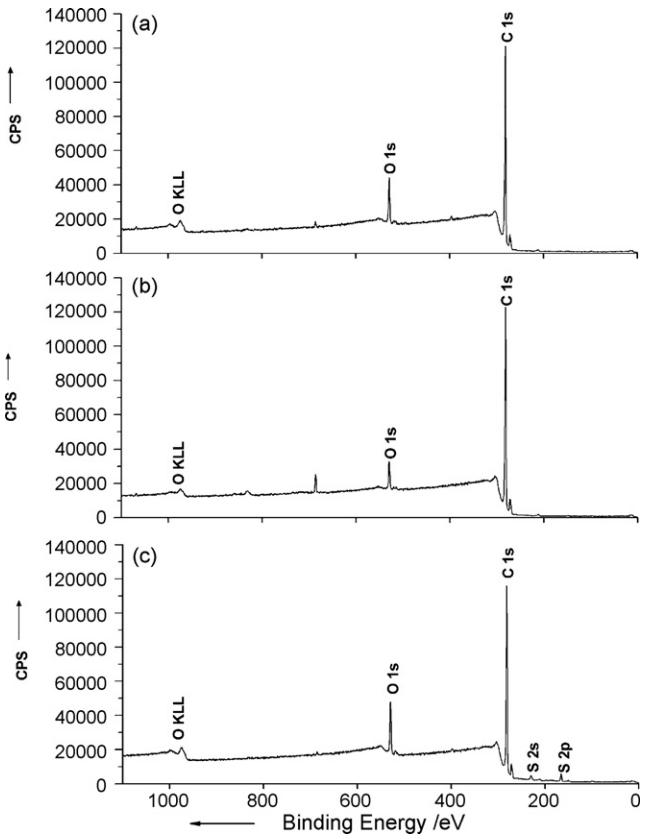

Fig. 1. XPS survey spectra of the (a) pristine UHMWPE, (b) 33% styrene-grafted UHMWPE and (c) 33% styrene-grafted and sulfonated UHMWPE 1.94 mequiv. g^{-1}.

was cut into sections 2.5 cm × 1.0 cm prior to being mounted in the cell. The cell was placed in a temperature controlled container open to air by a pinhole where the sample was equilibrated at 100% RH at ambient atmospheric pressure and clamped between two electrodes. The proton conductivities of the samples were measured in the longitudinal direction and were calculated from the impedance data, using the following relationship:

$$\sigma = \frac{l}{RS} \tag{3}$$

where σ is the proton conductivity (in S cm^{-1}), l is the distance between the electrodes used to measure the potential (l = 1.0 cm), S is the membrane cross-sectional surface area (membrane width × membrane thickness) for protons to transport through the membrane (in cm^2) and R is derived from the low intersection of the high frequency semicircle on a complex impedance plane with the Re (Z) axis.

2.7. Methanol permeability

Methanol permeability was measured using a simple two-compartment glass diffusion cell. A membrane (2.5 cm × 2.5 cm) was placed between two silicone rubber gaskets and with the two compartments clamped together around the gaskets. The active area of the membrane was 1.767 cm^2. Compartment A was filled with 100 mL of 10.0 vol.% methanol with an internal standard of 0.2 vol.% 1-butanol in aqueous solution. Compartment B was filled with 100 mL of 0.2 vol.% 1-butanol solution. The diffusion cell was placed in a water bath held at 30 °C, and each compartment was stirred by a separate stir plate to ensure uniform stirring. Samples (7 μL each) were removed from compartment B at intervals of ~20 min each. Methanol concentrations were determined by ^{1}H NMR spectroscopy. The methanol permeability was calculated [26].

2.8. Single cell DMFC test

The UHMWPE-g-PSSA membrane (DG = 22%) was selected for the DMFC testing. For this purpose, membrane was sprayed with catalyst with the final loading of 2 mg cm^{-2} Pt–Ru at the anode and 1 mg cm^{-2} Pt at the cathode side. Nafion® 5% solution (in lower aliphatic alcohol/H_2O mixture) was used as ionomer solution. Catalyst coated membrane was then sandwiched by anode and cathode electrodes, and hot-pressed at 90 °C under 2000 lbs pressure for 15 min. The obtained membrane–electrode assembly (MEA) was then sandwiched between two graphite current collectors with a serpentine design for the fuel and air distribution of 5 cm^2 geometrical active MEA area (Electrochem Inc.). Current, power and impedance values are normalized for the 5 cm^2 geometrical area. The single cell consisted of two ribbed graphite plates, which were compressed between two gold plated stainless steel plates. These plates were provided with liquid and gas-feed tubes and were connected with the electric wires for the measurements in the cell. Electrical heaters and a thermocouple were embedded into the plates to control the operating temperature of the FC. All electrochemical measurements were conducted in this cell. DMFC performance curves were measured at 40 and 60 °C.

2.8.1. Current–voltage curves

A peristaltic pump (Ismatec IPC 4, Cole-Parmer Inst. Co.) was employed to supply aqueous 1 M CH_3OH solutions to the anode at 2 mL min^{-1}. O_2 was fed to cathode at 100 sccm and at atmospheric pressure. O_2 was humidified by passing through a humidifier (Fuel Cell technologies) at 40 °C. Current–voltage curves were measured

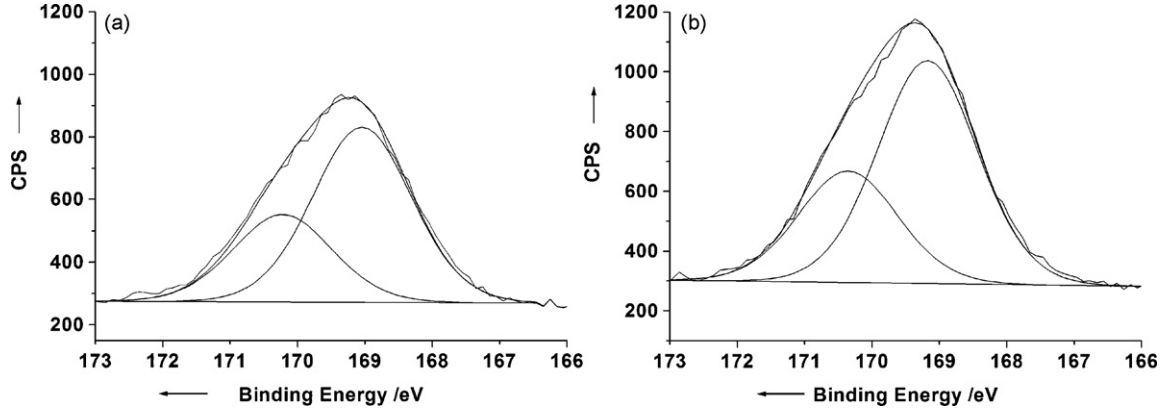

Fig. 2. High resolution XPS spectra and curve fitting of S $2p_{3/2}$ and S$2p_{1/2}$ from UHMWPE-g-PSSA: (a) DG = 22%, IEC = 1.5 mequiv. g^{-1}; (b) DG = 33%, IEC = 1.94 mequiv. g^{-1}.

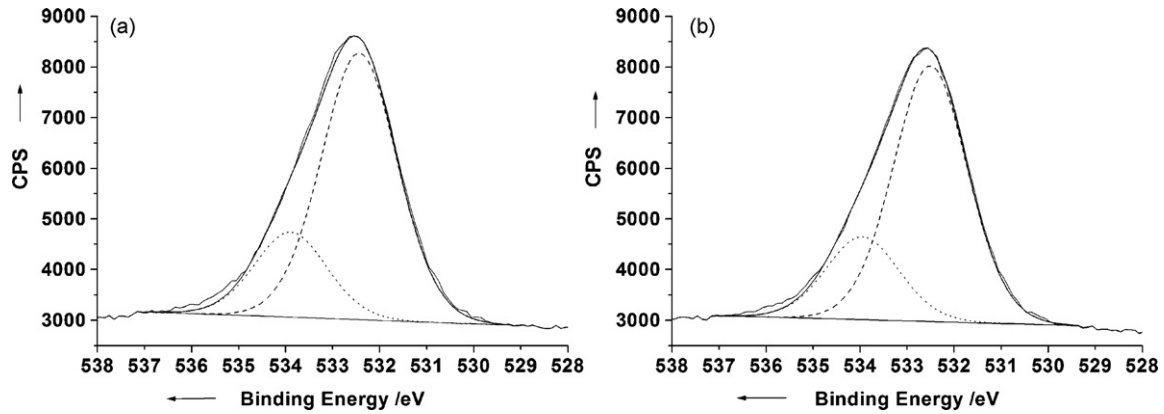

Fig. 3. High resolution XPS spectra and curve fitting of O 1s from UHMWPE-g-PSSA: (a) *DG* = 22%, *IEC* = 1.5 mequiv. g^{-1}; (b) *DG* = 33%, *IEC* = 1.94 mequiv. g^{-1}.

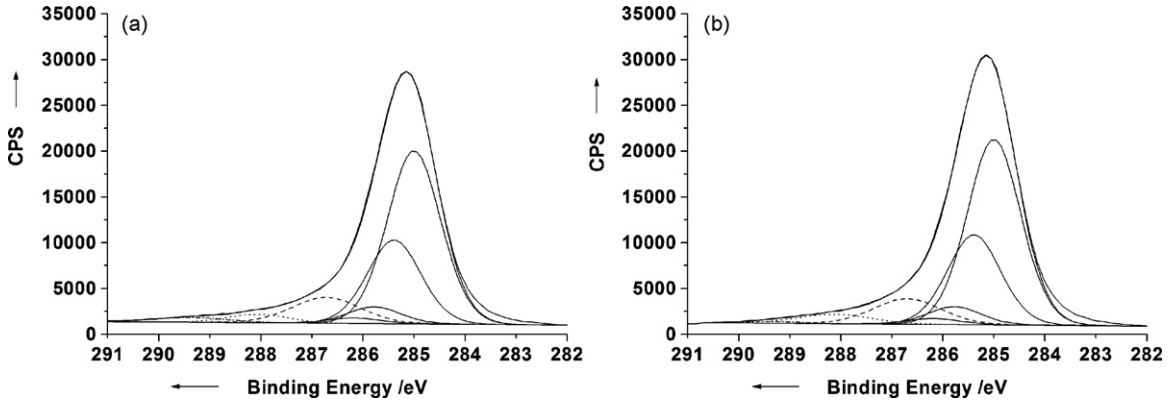

Fig. 4. High resolution XPS spectra and curve fitting of C 1s from UHMWPE-g-PSSA: (a) *DG* = 22%, *IEC* = 1.5 mequiv. g^{-1}; (b) *DG* = 33%, *IEC* = 1.94 mequiv. g^{-1}.

galvanostatically using an electronic load (Keithley 2440, Alliance Test Equipment, Inc.). Prior to the measurements, the cell was operated at 0.4 V and 40 °C for 2 h to condition the MEA. The cell performance was found to stabilize within 3 days of the measurements. The current–voltage polarization curves presented here were measured after 3 days of repeated conditioning and measuring the cell performance, unless otherwise stated.

3. Results and discussion

3.1. X-ray photoelectron spectroscopy (XPS)

Fig. 1 illustrates representative XPS survey spectra of the pristine UHMWPE, styrene-grafted UHMWPE (UHMWPE-g-PS), as well as sulfonated styrene-grafted UHMWPE (UHMWPE-g-PSSA). Strong, well-defined peaks at approximately 285 and 533 eV, indicative of C 1s and O 1s were observed in each survey scan. The strong C 1s peak at 285.0 eV, characteristic of C–C and C–H bonds, is shifted very slightly for UHMWPE-g-PS and UHMWPE-g-PSSA due to the presence of C=C in UHMWPE-g-PS and C=C and C–SO_3 in UHMWPE-g-PSSA. Deconvolution of the high resolution carbon spectra is discussed below. Weaker, poor signal-to-noise ratio, F and N peaks were found at 689.5 and 400.3 eV, respectively, in pristine UHMWPE (Fig. 1a) and styrene-grafted UHMWPE (Fig. 1b). The reason for their presence is unclear, but is thought to be due to environmental impurities.

Survey scans of the sulfonated styrene-grafted UHMWPE sample revealed a weak sulfur peak at approximately 169 eV (Fig. 1c). This confirmed the successful sulfonation of the styrene-grafted UHMWPE. The high resolution sulfur spectra (Fig. 2b) reveal S 2p present at a binding energy of 169.2 eV, which is consistent with oxidized sulfur (SO_3^-).

Fig. 1c shows the XPS survey spectrum of the sulfonated styrene-grafted UHMWPE (UHMWPE-g-PSSA) membranes as the PEMs. High resolution spectra of the PEMs reveal that, in addition to significant O 1s (Fig. 3b) and C 1s (Fig. 4b) peaks, a relatively weak S 2p peak was resolved at a binding energy of approximately 169 eV. This indicates that the membrane contains sulfonic acid groups. The possible presence of double bonds cannot be neglected during the styrene-grafting reaction [27]; therefore, it is possible that a side reaction took place when the membranes were sulfonated by chlorosulfonic acid. A possible side

Table 1
Calibrated binding energies for C 1s spectra of representative membranes.

Sample	*DG*/%	*IEC*/mequiv. g^{-1}	Binding energy						
			C–C, C–H				C–O (SO_3)	C=O	COOH
UHMWPE	0	0	285.0	285.4	285.8	286.2	286.7	288.2	289.4
UHMWPE-g-PS-33	33	0	285.0	285.4	285.8	286.2	286.7	288.1	289.3
UHMWPE-g-PSSA-22	22	1.5	285.0	285.4	285.8	286.2	286.7	288.0	289.4
UHMWPE-g-PSSA-33	33	1.94	285.0	285.4	285.8	286.2	286.7	288.2	289.5

Table 2
Atomic percent ratios based on XPS analyses for representative membranes.

Sample	*DG*/%	*IEC*/mequiv. g^{-1}	C/O	C/S	O/S
UHMWPE	0	0	12.7	–	–
UHMWPE-g-PS	33	0	16.2	–	–
UHMWPE-g-PSSA	22	1.5	12.2	69.6	5.7
UHMWPE-g-PSSA	33	1.94	10.6	41.1	3.9

reaction is the addition reaction of the chlorosulfonic acid with the double bonds on the grafts. The result of the side reactions is that there will be Cl atoms in the sulfonated membranes; however, no detectable Cl was observed in the survey spectra. Hence, if indeed there are double bonds present in the grafted membrane, which will react with chlorosulfonic acid during sulfonation, the amount present is below the level detectable by XPS.

Fig. 2 shows the XPS high resolution spectra and curve fitting of the UHMWPE-g-PSSA membranes. The peak area increases with increasing degree of grafting, as illustrated by the S 2p signal of the

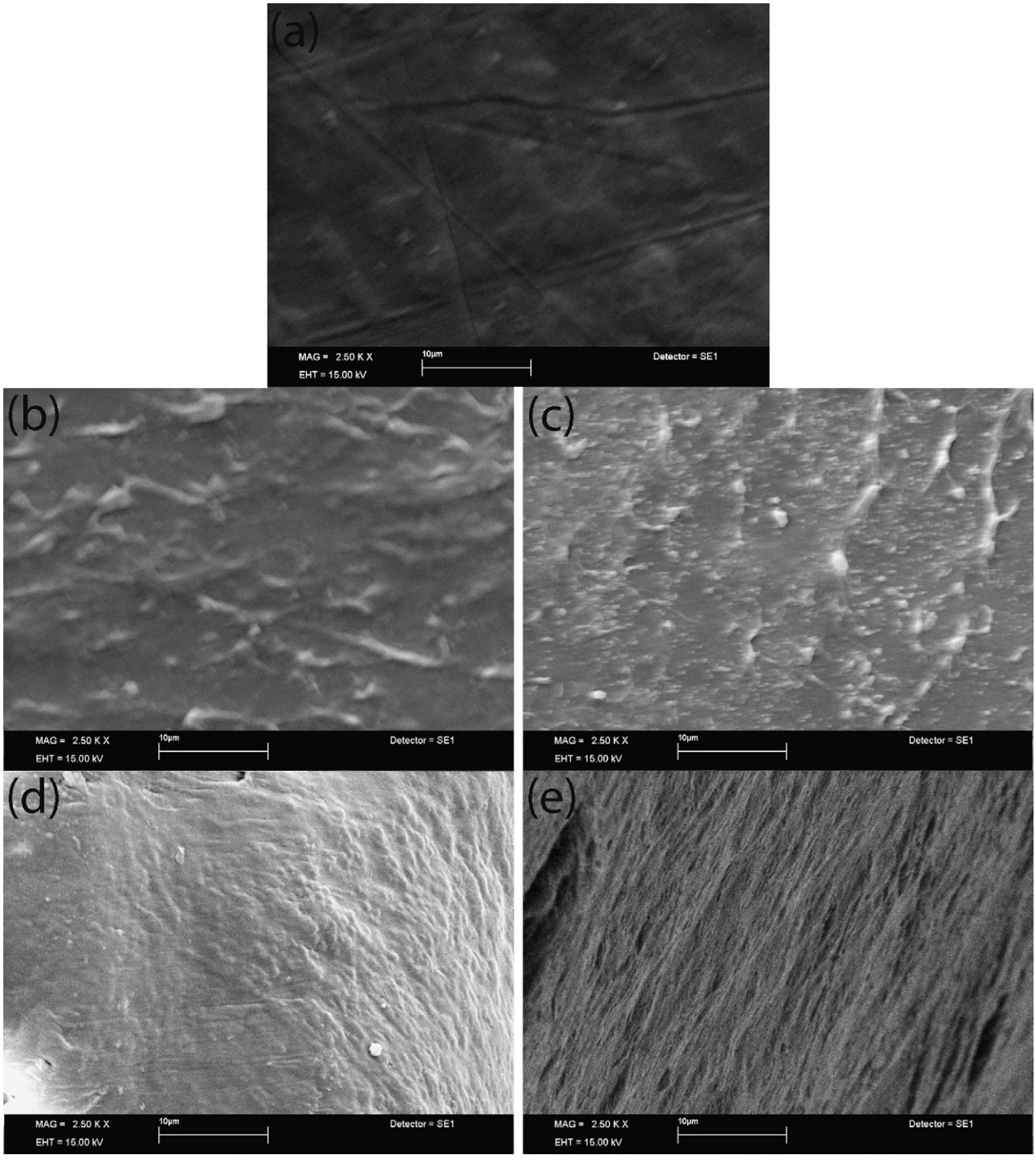

Fig. 5. SEM micrographs at magnification = 2500×: (a) pristine UHMWPE; (b) UHMWPE-g-PS (*DG* = 33%); (c) UHMWPE-g-PSSA (*DG* = 33%); (d) cross-sections of UHMWPE-g-PS (*DG* = 33%); (e) cross-sections of UHMWPE-g-PSSA (*DG* = 33%).

33% sulfonated styrene-grafted UHMWPE (Fig. 2b) versus the same signal for the respective 22% membrane (Fig. 2a).

The carbon spectra were fitted based on the fitting of high density polyethylene (PE) and polystyrene (PS) provided by Beamson and Briggs [25] and Lukas and Tyrackova [28]. The high resolution carbon spectra were typically fitted with synthetic curves having a full width half maximum of 1.2 eV. The O 1s spectra (Fig. 3a and b) have been fitted with the oxygen peak at 532.5 which is attributed to oxygen of sulfonic acid group.

There is a high degree of overlap between the carbon peaks, making them virtually indistinguishable. Peaks 1–4 represent vibrational fine structure with the higher binding energy components due to low-level oxidation [25]. The higher energy C 1s peaks are consistent with peak fittings by Lukas and Tyrackova [28] of PE and PS. Synthetic peak position, peak assignments, atomic percent and atomic ratio calculation are summarized in Tables 1 and 2.

3.2. Scanning electron microscope (SEM) studies

The SEM images were obtained by using compression moulded films of pure UHMWPE, UHMWPE-g-PS and sulfonated UHMWPE-g-PS. The surface of pure UHMWPE films (Fig. 5a) is observed to be smooth with no observable discontinuity, indicating complete melting and flow. Thus compression moulding is an appropriate technique for film formation of UHMWPE, which is insoluble in almost any solvent. However, there is possible difference in the melt temperature of pristine and styrene-grafted UHMWPE. Therefore, the temperature applied during compression moulding of UHMWPE-g-PS was maintained higher well above the melting point of pristine UHMWPE.

Fig. 5b shows the image of film prepared from 33% styrene-grafted UHMWPE powder. The appearance of surface roughness is due to the presence of PS grafts. A few distinctive particles with macroscopic phase separation also appear that can be attributed to the possible presence of some non-melted portion of highly grafted UHMWPE-g-PS powder. However, the accumulation of the styrene graft on the surface of the film is not observed, which is considered as a significant advantage of employing the post-grafting film formation from UHMWPE-g-PS powder, as opposed to grafting onto pre-formed films. The accumulation of graft units on the surface can cause film brittleness; moreover, inhomogeneous penetration of the grafting units throughout the volume of film contributes to a higher resistance in transfer of conducting ions through the film, which would adversely affect the PEM. UHMWPE-g-PS films were sulfonated with chlorosulfonic acid to convert them to proton conducting membranes. SEMs of selected UHMWPE-g-PSSA membranes are illustrated in Fig. 5c. In comparison with UHMWPE-g-PS, no new features were observed in the UHMWPE-g-PSSA membranes other than the significant increase in surface roughness, which may be due to the swelling effect brought about by sulfonation of the film.

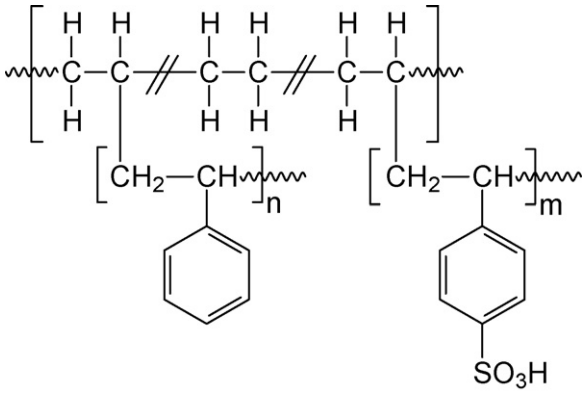

Fig. 6. Representative structure of UHMWPE-g-PSSA.

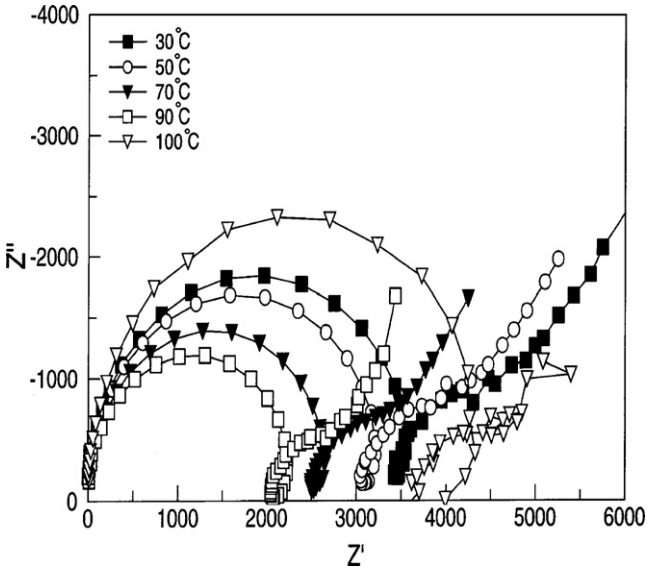

Fig. 7. AC impedance spectra for UHMWPE-g-PSSA membrane (*DG* = 12%, *IEC* = 0.97 mequiv. g^{-1}).

Fig. 5d and e shows the cross-sectional view of the UHMWPE-g-PS and UHMWPE-g-PSSA membranes, respectively. The micrograph shows that PS grafts are present not only on the surface of the film but throughout the volume of the membrane, which confirms the uniformity of grafting and then sulfonation process during PEMs development.

3.3. Proton conductivity/methanol permeability

Membranes for use in DMFC systems must possess both adequate proton conductivity and be effective barriers for methanol crossover from the anode to the cathode, to prevent loss of methanol and oxidation with oxygen, leading to a mixed potential. Proton conduction is due to the presence of protogenic groups,

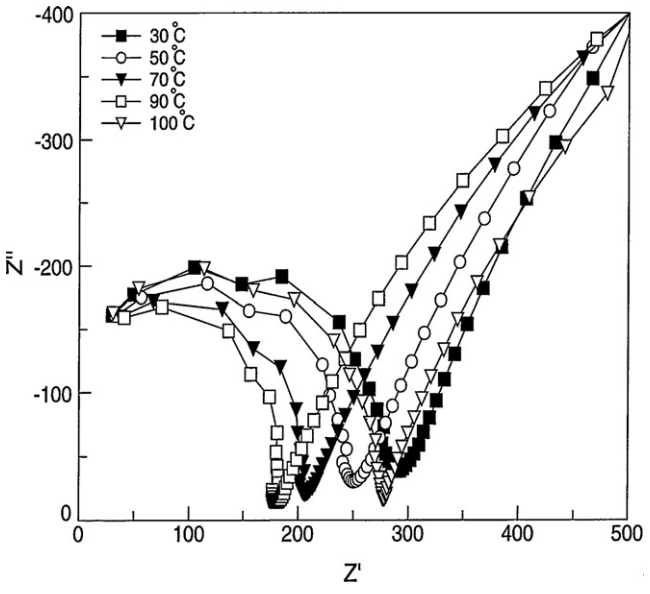

Fig. 8. AC impedance spectra for UHMWPE-g-PSSA membrane (*DG* = 44%, *IEC* = 2.26 mequiv. g^{-1}).

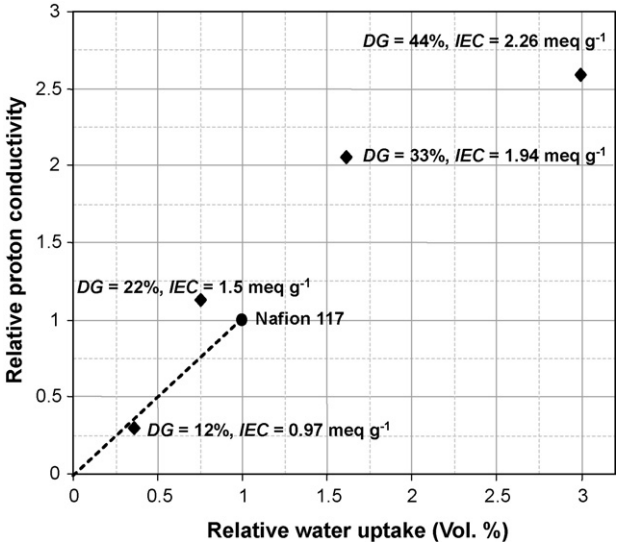

Fig. 9. Proton conductivity versus water uptake (vol.%) of UHMWPE-g-PSSA relative to Nafion® 117.

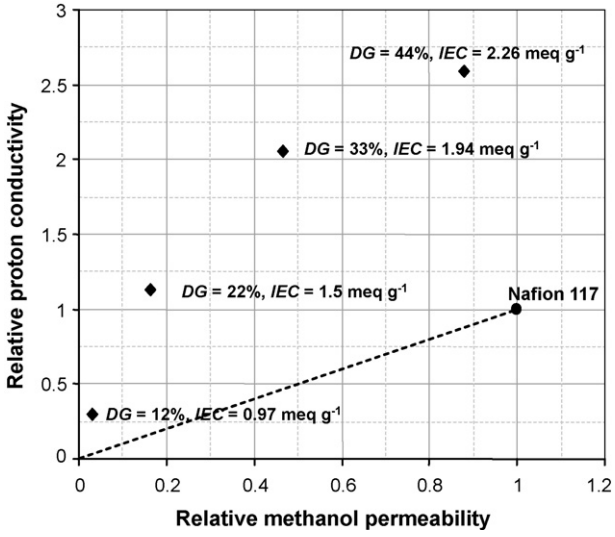

Fig. 10. Proton conductivity versus methanol permeability of UHMWPE-g-PSSA relative to Nafion® 117.

and UHMWPE-g-PSSA contains sulfonic acid groups that afford proton conduction. The structure of UHMWPE-g-PSSA is represented in Fig. 6.

In addition to the presence of sulfonic acid groups as protogenic group, in the case of Nafion®, its interconnected ionic domains strongly contribute to its high proton conductivity, but at the same time contribute to fast methanol diffusion. High methanol crossover is a significant drawback of Nafion® in the DMFC application. Methanol transport and proton conductivity often have a trade-off relationship, whereby it is difficult to selectively reduce one without affecting the other.

Nasef et al. [29] and Gubler et al. [30] outlined in detail the problems encountered during proton conduction measurements for the grafted PEMs, in which grafting was conducted on polymer film substrates. It was described that at low *DG*, the polystyrene grafts are located near the surface of the film while the membrane interior remains ungrafted and subsequently exerts a high local resistance to proton conduction due to inhomogeneous distribution of ion exchange sites over the area of the membrane. Thus the conductivity data obtained from their results show considerable scatter at low and medium *DG* values of ≤20%, because the AC impedance spectra obtained were of poor quality and unsuitable for the extraction of meaningful numbers. Gubler et al. also confirmed the inhomogeneous distribution of ion exchange sites over the area of the membrane by observing the patchy coloring of the membranes upon the introduction of an indicator dye. It was also described that the membranes became increasingly brittle at higher graft levels, and thus could not even be used for conductivity measurements because of fracturing. Both of these challenges (1) penetration of graft throughout the membrane and (2) brittleness for high *DG* films, are adequately addressed in the present study by applying a new fabrication protocol, i.e., irradiation grafting modification of the base polymer in the powder, subsequent film fabrication and post-sulfonation. The present methodology considerably improved the uniformity of grafting distribution throughout the film cross-sectional volume and is confirmed by the continuity in conductivity data. The impedance curves obtained even for the membrane with lower *DG*, i.e., UHMWPE-g-PSSA having a *DG* of 12% were of better

Table 3
Comparison of proton conductivities of PEMs based on radiation induced styrene-grafted copolymers.

Base polymer	Thickness/μm	Monomer	*DG*/mass%	Proton conductivity/mS cm^{-1}	Ref.
UHMWPE	90[a]	Styrene	12	16[b]	–
UHMWPE	92[a]	Styrene	22	61[b]	–
UHMWPE	102[a]	Styrene	33	111[b]	–
UHMWPE	122[a]	Styrene	44	140[b]	–
Nafion® 117	176[a]	Styrene	–	54[b]	[26]
PVDF	80[c]	Styrene	36–39	50[d]	[31,32]
PVDF	40[c]	Styrene	39	48[d]	[31,32]
PVDF	15[c]	Styrene	36	16[d]	[31,32]
ETFE	50[c]	Styrene	36–39	43[d]	[31,32]
FEP	75[c]	Styrene	34	108[d]	[31,32]
PTFE	35[c]	Styrene	16	70[e]	[33,34]
FEP(R-4010)	75[a]	Styrene	22	90[e]	[33,34]
LDPE(R-5010M)	195[a]	Styrene	16	30[e]	[33,34]
LDPE	125[c]	Styrene	9	54[f]	[35,36]
ETFE	50[c]	Styrene	14	18[f]	[35,36]
PFA	120[c]	Styrene	16	33[d]	[37]

[a] Thickness of grafted and sulfonated membrane.
[b] At 35 °C and 100% RH.
[c] Thickness of base polymer film.
[d] At room temperature and 100% RH.
[e] In situ in cell of 5 cm^2 activated area, 50 °C, H_2/O_2 at 4/5 atm, full humidification.
[f] At room temperature in 0.1 M HCl.

quality as shown in Fig. 7. This further improved with *DG* as excellent impedance curves were obtained for UHMWPE-g-PSSA having *DG* of 44%, as shown in Fig. 8.

Fig. 9 shows that the proton conductivity and water uptake are interrelated properties. Water uptake value of UHMWPE-g-PSSA membranes increases gradually with increase in *IEC*. This increase in water uptake leads to increased proton conduction due to reason that H_2O act as proton carrier, as H^+ conducts in the form of H_3O^+ or $H_2O_5^+$ through the membrane. Fig. 10 shows that the proton conductivity of the UHMWPE-g-PSSA membranes increases with *DG* and *IEC* but at the same time the methanol permeability value also increases undesirably. Due to this trade-off relationship between methanol permeability and proton conductivity, it is of little value to select a membrane having very high *IEC*. Thus the membrane of choice will be that which bears low methanol permeability along with reasonably high proton conductivity.

Selectivity, which is defined as the ratio of proton conductivity to methanol permeability, is often used to evaluate the potential performance of polymeric films. Figs. 9 and 10 also present the relative values of proton conductivity, water uptake and methanol permeability of UHMWPE-g-PSSA membranes to Nafion® 117. It was found that UHMWPE-g-PSSA membranes have higher selectivities compared to Nafion® 117. The methanol permeability of UHMWPE-g-PSSA at 30 °C were in the range of 1.45×10^{-6} to 4.86×10^{-8} cm^2 s^{-1}, several times lower than the methanol permeability of Nafion® 117 (1.5×10^{-6} cm^2 s^{-1}).

For the purpose of comparison, the proton conductivity of few PEMs based on radiation induced styrene-grafted onto different base polymers are presented along with the measurement conditions in Table 3. As it was observed that in most cases, grafting studies were performed using fluorinated base polymers which are costly and environmentally unfriendly contrary to UHMWPE, being purely hydrocarbon. Moreover, UHMWPE-g-PSSA has an excellent proton conductivity.

3.4. DMFC performance of UHMWPE-g-PSSA membrane

The UHMWPE-g-PSSA membrane (*DG* = 22%, 92 μm thickness) was selected for evaluation of the DMFC performance, due to its considerably lower methanol permeability together with satisfactory proton conductivity and water uptake, as shown in Figs. 9 and 10. The fabricated single cell was fed with 1 M aqueous methanol to the anode and O_2 to the cathode, under atmospheric pressure. After the cell attained stable conditions, the current–voltage (*I–V*) performance of the cell was recorded at 40 and 60 °C. For comparison, Nafion® 117 (176 μm thickness) was also tested under the same conditions, and the results are presented in Figs. 11 and 12.

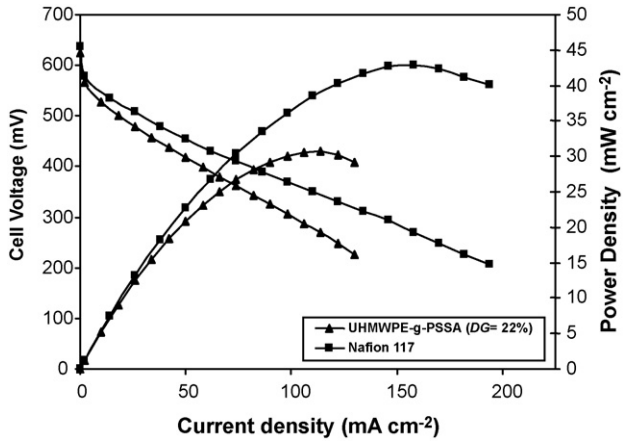

Fig. 11. DMFC performance of UHMWPE-g-PSSA (*DG* = 22%) compared to Nafion® 117 at 40 °C.

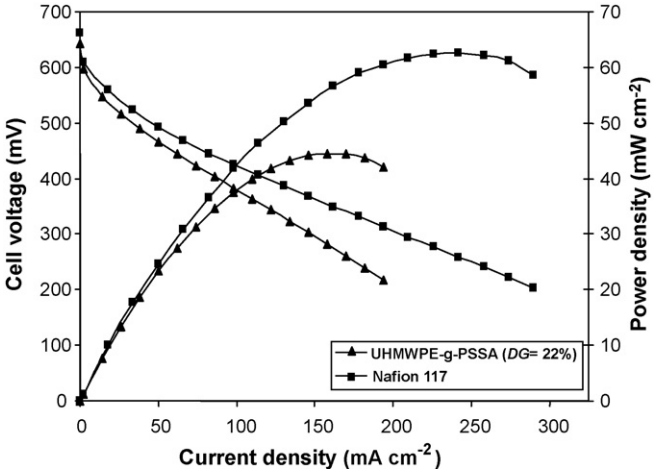

Fig. 12. DMFC performance of UHMWPE-g-PSSA (*DG* = 22%) compared to Nafion® 117 at 60 °C.

The open cell voltage (OCV) values of the membrane increases slightly at higher temperature that is possibly due to the decrease in resistance for cations movement through the membranes while methanol permeability as already checked is very low. In all graphs, there are clear regions of activation, ohmic and concentration polarization. The activation and ohmic polarization is significant at 40 °C, but becomes lower at 60 °C while the portion of the curves representing concentration polarization are almost similar at both temperatures. By comparing the power density curves of the membranes at 40 and 60 °C temperatures (see Fig. 11) it is obvious that UHMWPE-g-PSSA membrane shows superior performance at higher temperature at every low and high current density regions of the curves.

Since Nafion® ionomer was used for MEA fabrication and the UHMWPE-g-PSSA membrane is purely hydrocarbon, it would be expected that compatibility between the membrane and ionomer would compromise the connectivity of the membrane–electrode. However, smooth polarization curves were obtained, and the power density is comparable to that of Nafion®. With optimization of the membrane–electrode interface and further improvements in MEA fabrication, it is likely that the performance could be improved. Furthermore, due to the significantly lower methanol crossover,

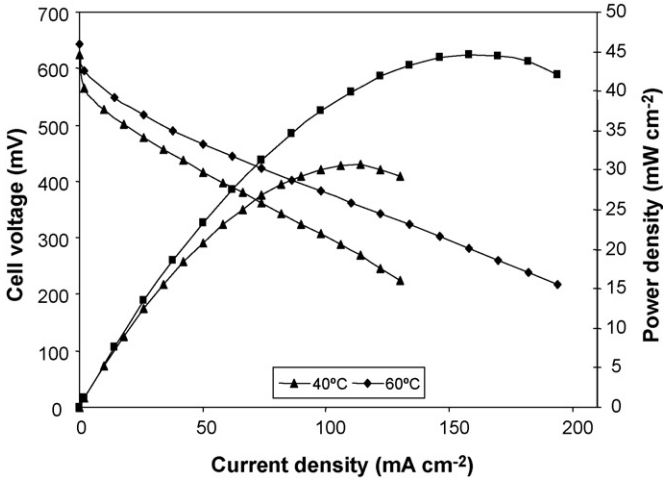

Fig. 13. Variation in DMFC performance of UHMWPE-g-PSSA (*DG* = 22%) at different temperatures.

the performance of UHMWPE-g-PSSA membrane could also be improved by its use in a DMFC with higher methanol feed concentration, while the performance of Nafion® membranes in DMFC declines when the methanol feed concentration exceeds 2 M, due to high methanol crossover [38]. Fig. 13 shows that the DMFC performance of UHMWPE-g-PSSA is improved with increasing temperature. This trend supports the appropriate connectivity of the ionic sites throughout the volume of the membrane, which results in higher conductivity with increasing temperature. The power density of UHMWPE-g-PSSA (DG = 22%) membrane obtained was about 32 mW cm^{-2} at 40 °C to 45 mW cm^{-2} at 60 °C.

4. Conclusions

Fuel cell membranes based on styrene-grafted polyethylene were successfully prepared. The sulfonation was confirmed by XPS spectroscopy. SEM analysis confirmed that compression moulded films of the pre-styrene-grafter polymer UHMWPE-g-PS could be suitably prepared with essentially pore-free and homogeneous structures. The resulting films were post-sulfonated to provide grafted membranes having comparable or higher proton conductivity and lower methanol permeability than Nafion® 117 membrane. The DMFC test demonstrated the practicability of using these membranes, as smooth polarization curves were obtained. UHMWPE-g-PSSA is an inexpensive membrane material and hence is a viable alternate to Nafion® for DMFCs applications.

Acknowledgments

The authors wish to gratefully acknowledge the financial support of Higher Education Commission (HEC) of Pakistan for this project. Mr. Maqsood Ahmad from PINSTECH, Islamabad, Pakistan is thanked for assistance with SEM analysis.

References

[1] B.C.H. Steele, A. Heinzel, Nature (London) 414 (2001) 345.
[2] M. Rikukawa, K. Sanui, Prog. Polym. Sci. 25 (2000) 1463.
[3] M.A. Hickner, H. Ghassemi, Y.S. Kim, B.R. Einsla, J.E. McGrath, Chem. Rev. 104 (2004) 4587.
[4] Y. Yang, S. Holdcroft, Fuel Cells 5 (2005) 171.
[5] P.L. Antonucci, A.S. Arico, P. Creti, E. Ramunni, V. Antonucci, Solid State Ionics 125 (1999) 431.
[6] P. Dimitrova, K.A. Friedrich, B. Vogt, U. Stimming, J. Electroanal. Chem. 532 (2002) 75.
[7] J.-C. Lin, M. Ouyang, J.M. Fenton, H.R. Kunz, J.T. Koberstein, M.B. Cutlip, J. Appl. Polym. Sci. 70 (1998) 121.
[8] J.A. Kerres, J. Membr. Sci. 185 (2001) 3.
[9] K. Miyatake, Y. Chikashige, M. Watanabe, Macromolecules 36 (2003) 9691.
[10] K.D. Kreuer, J. Membr. Sci. 185 (2001) 29.
[11] J.H. Fang, X.X. Guo, S. Harada, T. Watari, K. Tanaka, H. Kita, K. Okamoto, Macromolecules 35 (2002) 9022.
[12] K. Miyatake, N. Asano, M. Watanabe, J. Polym. Sci. A: Polym. Chem. 41 (2003) 3901.
[13] E.J. Powers, G.A. Serad, High Performance Polymers: Their Origin and Development, Elsevier, Amsterdam, 1986, p. 355.
[14] L. Wang, Y.Z. Meng, S.J. Wang, X.Y. Shang, L. Li, A.S. Hay, Macromolecules 37 (2004) 3151.
[15] Y. Gao, G.P. Robertson, M.D. Guiver, S.D. Mikhailenko, X. Li, S. Kaliaguine, Macromolecules 38 (2005) 3237.
[16] T. Kobayashi, M. Rikukawa, K. Sanui, N. Ogata, Solid State Ionics 106 (1998) 219.
[17] H. Ghassemi, J.E. McGrath, Polymer 45 (2004) 5847.
[18] D.J. Jones, J. Roziere, J. Membr. Sci. 185 (2001) 41.
[19] R.K. Nagarale, G.S. Gohil, V.K. Shahi, R. Rangarajan, Macromolecules 37 (2004) 10023.
[20] T.R. Dargaville, G.A. George, D.J.T. Hill, A.K. Whittaker, Prog. Polym. Sci. 28 (2003) 1355.
[21] M.M. Nasef, E. Hegazy, Prog. Polym. Sci. 29 (2004) 499.
[22] T. Yamaguchi, F. Miyata, S. Nakao, J. Membr. Sci. 214 (2003) 283.
[23] B. Baea, H.Y. Hab, D. Kima, J. Membr. Sci. 276 (2006) 51.
[24] T.A. Sherazi, S. Ahmad, M.A. Kashmiri, M.D. Guiver, J. Membr. Sci. 325 (2008) 964.
[25] G. Beamson, D. Briggs, High Resolution XPS of Organic Polymers: The Scienta ESCA300 Database, John Wiley and Sons, Inc., 1992.
[26] T.A. Sherazi, S. Ahmad, M.A. Kashmiri, D.S. Kim, M.D. Guiver, J. Membr. Sci. 333 (2009) 59.
[27] J. Li, S. Ichizuri, S. Asano, F. Mutou, S. Ikeda, M. Iida, T. Miura, A. Oshima, Y. Tabata, M. Washio, Appl. Surf. Sci. 245 (2005) 260.
[28] J. Luckas, V. Tyrackova, J. Membr. Sci. 58 (1991) 49.
[29] M.M. Nasef, H. Saidi, H.M. Nor, O.M. Foo, J. Appl. Polym. Sci. 78 (2000) 2443.
[30] L. Gubler, N. Prost, S.A. Gürsel, G.G. Scherer, Solid State Ionics 176 (2005) 2849.
[31] T. Kallio, M. Lundstrom, G. Sundholm, N. Walsby, F. Sundholm, J. Appl. Electrochem. 32 (2002) 11.
[32] T. Kallio, K. Jokela, H. Ericson, R. Serimaa, G. Sundholm, P. Jacobsson, F. Sundholm, J. Appl. Electrochem. 33 (2003) 505.
[33] A.G. Guzman-Garcia, P.N. Pintauro, M.W. Verbrugge, E.W. Schneider, J. Appl. Electrochem. 22 (1992) 204.
[34] H. Wang, G.A. Capuano, J. Electrochem. Soc. 145 (1998) 178.
[35] J.A. Horsafall, K.V. Lovell, Fuel Cells 1 (2001) 186.
[36] J.A. Horsafall, K.V. Lovell, Polym. Adv. Technol. 13 (2002) 381.
[37] M.M. Nasef, H. Saidi, J. New Mater. Electrochem. Syst. 5 (2002) 183.
[38] X. Ren, T.E. Springer, S. Gottesfeld, J. Electrochem. Soc. 147 (2000) 92.